Hindawi Publishing Corporation
International Journal of Antennas and Propagation
Volume 2008, Article ID 378285, 7 pages
doi:10.1155/2008/378285

Research Article

Archimedean Spiral Antenna Calibration Procedures to Increase the Downrange Resolution of a SFCW Radar

Ioan Nicolaescu[1] and Piet van Genderen[2]

[1] *Department of Military Electronic Systems and Communications, Military Technical Academy, 81-83 George Cosbuc Avenue, Bucharest 050141, Romania*
[2] *International Research Centre for Telecommunication-transmission and Radar, University of Technology, Mekelweg, 2628 Delft, The Netherlands*

Correspondence should be addressed to Ioan Nicolaescu, ioannic@mta.ro

Received 18 June 2007; Revised 5 October 2007; Accepted 12 February 2008

Recommended by Dejan Filipovic

This paper deals with the calibration procedures of an Archimedean spiral antenna used for a stepped frequency continuous wave radar (SFCW), which works from 400 MHz to 4845 MHz. Two procedures are investigated, one based on an error-term flow graph for the frequency signal and the second based on a reference metallic plate located at a certain distance from the ground in order to identify the phase dispersion given by the antenna. In the second case, the received signal is passed in time domain by applying an ifft, the multiple reflections are removed and the phase variation due to the time propagation is subtracted. After phase correction, the time domain response as well as the side lobes level is decreased. The antenna system made up of two Archimedean spirals is employed by SFCW radar that operates with a frequency step of 35 MHz.

1. INTRODUCTION

Located at the interface between the propagation media and the electronic device, the antenna is a very important element of any electronic equipment used either to pass information from one place to another or for object detection and tracking (radar systems etc.). In the last decade, a lot of work has been done to find a proper system for landmine detection. Among other systems, the ground penetrating radar (GPR) is very promising because of its advantages over other types of sensors as: no direct contact with the surface, the possibility to detect both metallic and nonmetallic objects, and so forth. The GPR works either in time domain (video pulse radar) or in frequency domain (SFCW radar). In the case of SFCW radar, the antenna system consists of two antennas, one for transmission and the other one for reception, which will be moved above the ground at a certain distance (in this specific case 70 cm) to scan the ground surface. The main parameters of radar are the range and the resolution. The range of SFCW radar is given by the frequency step and the resolution by the frequency range. For landmine detection, one needs both deep penetration and high resolution. Taking into account these requirements and the international regulations with regards to frequency allocation, the frequency range for SFCW radar has been chosen from 400 MHz to 4845 MHz. The low frequency will provide deep penetration while high frequency will give the needed resolution. The antenna system has to comply with these frequency range, has to have a stationary phase point because the distance is phase embedded, and should have no extra delays within the antenna because they will worsen the down range resolution of the system. Moreover, because the system is a bistatic one (one antenna for transmission and one antenna for reception, 52 cm apart), the coupling signal and the common footprint have to be as low as possible to provide both dynamic range and cross-range resolution. Several ultra wideband (UWB) antennas had been investigated for this application and the best fit was found for two Archimedean spirals with opposite sense of rotation that have a low level of the leakage signal and provide circular polarization, which is a very important advantage in this application. However, the Archimedean spiral has a frequency dependent delay that will worsen the range resolution. In order to remove the delay, two procedures are investigated in this paper.

2. ANTENNA SYSTEM—TIME DOMAIN RESPONSE

In order to identify the delay within the antenna systems, the two Archimedean antennas had been connected to a vector network analyzer (VNA) set to work as an SFCW radar from 400 MHz to 4845 MHz in 128 steps (the frequency step was 35 MHz). One antenna will transmit 128 frequencies and the other will receive the reflected signals.

If a metallic plate is placed at a distance d of the antenna system and the power transmitted by the radar is equalized for all 128 frequencies, then the transmitted signalcan be written like

$$u(t) = \frac{1}{128}\sum_{n=1}^{128} A e^{j2\pi f_n t}, \quad (1)$$

where A is a constant. This signal propagates to the metallic plate and is scattered back to the antenna system. The received signal can be written as

$$s(t, t_{in}) = \frac{1}{128}\sum_{n=1}^{128} r_n A e^{j2\pi f_n (t - t_{in})}, \quad (2)$$

where t_{in} denotes the delay due to the antenna system and due to propagation towards the metallic plate and back; r_n includes the propagation losses as well as the reflection losses.

The delay t_{in} is frequency dependent because the delays within the antenna system depend on frequency [1]. This happens due to the principle of operation of spiral antenna, which states that this antenna has an active part that changes with frequency such as the ratio between the geometrical dimension and the wavelength stays constant. The lower frequencies have a larger delay than the higher frequencies [2] because at lower frequencies, the currents have to propagate a longer way before being radiated than the currents at higher frequencies. This will lead to an increased time response as can be seen in Figures 1–3, where three situations are displayed.

The first one corresponds to the case when the ifft transform is applied to a set of 128 frequencies that cover the entire operational band of the radar and the synthesized time response is about 9 nanoseconds. The second case is for 108 frequencies (first 20 frequencies are removed) and the synthesized time response is around 5.5 nanoseconds. In the third situation, the last 20 frequencies are removed and the synthesized time response is about 8.5 nanoseconds.

The signals for the three situations are given by

$$s_1(t_{in}) = \frac{1}{128}\sum_{n=1}^{128} r_n A e^{-j2\pi f_n t_{in}}; \quad (3)$$

for all 128 frequencies,

$$s_2(t_{in}) = \frac{1}{108}\sum_{n=21}^{128} r_n A e^{-j2\pi f_n t_{in}}; \quad (4)$$

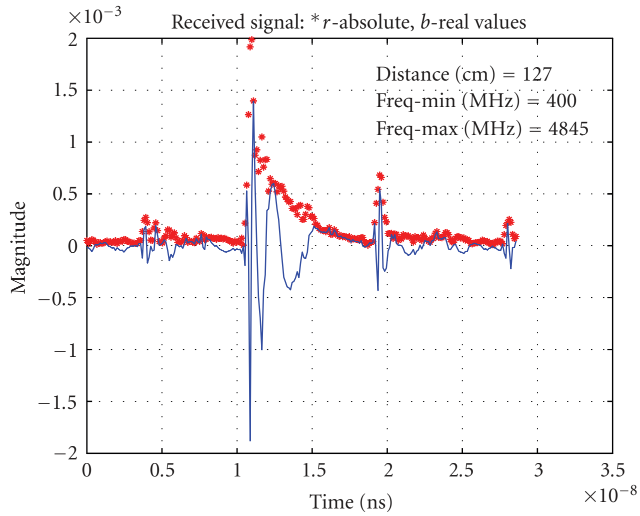

FIGURE 1: The received signals, in time domain, for 4445 MHz frequency span (128 frequencies).

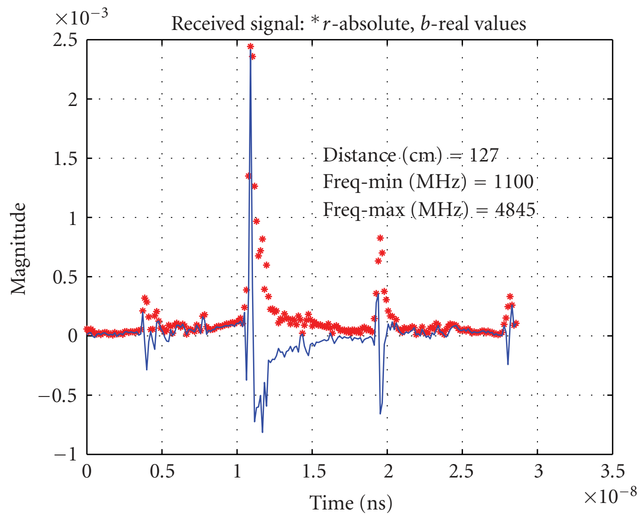

FIGURE 2: The received signals, in time domain, for 3745 MHz frequency span (108 frequencies—first 20 removed).

for 108 frequencies (first 20 removed), and

$$s_3(t_{in}) = \frac{1}{108}\sum_{n=1}^{107} r_n A e^{-j2\pi f_n t_{in}}; \quad (5)$$

for 108 frequencies (last 20 removed), where $0 \le t_{in} \le 1/\triangle f$.

3. CALIBRATION USING AN ERROR-TERM FLOW GRAPH

3.1. Formulation

The time response of the antenna system is drastically increased due to different delays associated with different frequencies (Figures 1–3). The calibration procedure should remove this phase dispersion introduced by the antenna system. Because the radar measures amplitude and phase,

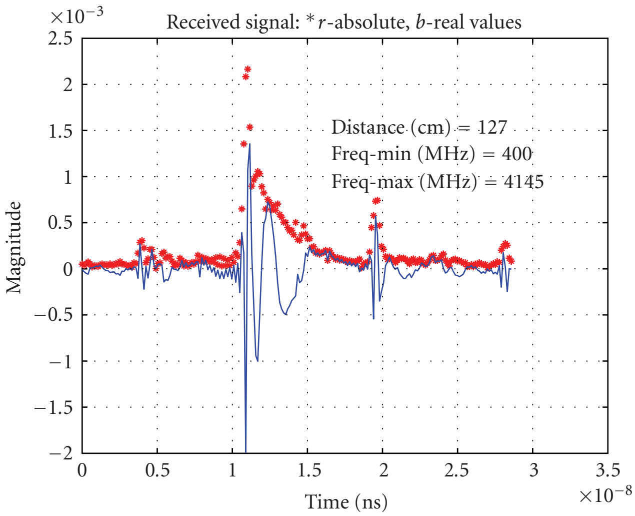

Figure 3: The received signals, in time domain, for 3745 MHz frequency span (108 frequencies—last 20 removed).

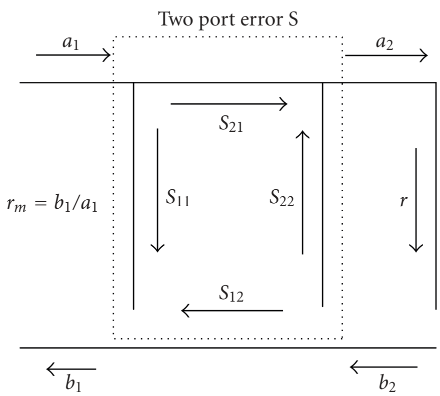

Figure 4: Error-term flow graph for one port vector network analyzer; a and b are reflected waves.

in other words, it is a vectorial device, the calibration procedure that is in place for vector network analyser should be followed. A vector network analyser is calibrated by using an error-term flow graph for the frequency signal like in Figure 4.

The reflection coefficient r, which is a function of frequency, can be calculated using the well-known formula [3]

$$r = \frac{r_m - S_{11}}{S_{12}S_{21} - S_{22}(r_m - S_{11})}. \tag{6}$$

The three unknowns (S_{11}, S_{22}, and $S_{12}S_{21}$) in (6) can be determined by measuring the reflections from three standards, which for vector network analyzer are: the open, the short, and the matched load. If we are able to find the three standards, this procedure can be used for calibration.

In order to apply this procedure to SFCW radar, let us assume that all systematic linear errors are included in the two-port error network. The correct reflection coefficient, r, from an object will be given by formula (6), where S_{11} represents the leakage signal and S_{22} depends on the radar cross section (RCS) of the antenna and takes into account the multiple ground bounces. The three unknowns can be computed if three independent calibration targets are available. According to [4], these are represented by free space ("empty room," $r = 0$), a metal plate ($r = -1$), and a wire grid. The error coefficients can be derived as follows:

$$S_{11} = r_{mo},$$
$$S_{22} = \frac{r_{mg} - r_{mo} + r_g(r_{mg} - r_{mo})}{r_g(r_{mg} - r_{mm})}, \tag{7}$$
$$S_{12}S_{21} = -(r_{mg} - r_{mo})(1 + S_{22}),$$

where r_{mo}, r_{mm}, and r_{mg} denote measured signals for "empty room," metal plate, and metal grid and r_g is the exact reflection coefficient of the metal grid. Having the error coefficients, the reflection coefficient for any object can be easily computed using (7).

The disadvantage of this procedure lies in the difficulty to find the precise value of the reflection coefficient for the third standard (wire grid). It can be found either by measurements or by calculation. V. Mikhnev has proposed a procedure that replaces the third standard by measuring the reflection coefficient from the same metallic plate placed in one or several shifted locations. If the reflectivity of the antenna system from the free space is low ($S_{22} \ll 1$), which is true when the antenna system is high enough above the ground, then the reflection coefficient of the shifted metal plate can be written as

$$r_{sp}(f) = r_m(u + vf + wf^2)\exp(-j2\beta l), \tag{8}$$

where r_{sp} is the reflection coefficient of the metallic plate placed in a shifted position; l is the offset distance, β is the phase propagation constant and u, v, and w are parameters which depend on l. If S_{22} is neglected then, the real value of the reflection coefficient can be computed using the formula

$$r = \frac{r_m - S_{11}}{S_{12}S_{21}}, \tag{9}$$

and the unknown parameters u, v, and w can be determined by solving the optimization problem

$$\sum_n \left| \frac{r_{sp}(f_n) - r_o(f_n)}{r_m(f_n) - r_o(f_n)} - (u + vf_n + wf_n^2)\exp(-j2\beta_n l) \right| \longrightarrow \min. \tag{10}$$

3.2. Experimental results

Having the values of the unknown parameters in (8), the exact value of the reflection coefficient of the shifted metallic plate can be computed. This method provides better results if the offset distance is around a quarter of a wavelength. The SFCW radar is an ultra wideband device; it operates from 400 to 4845 MHz so it is not possible to make measurements at a quarter of wavelengths for all frequencies. This is why several measurements have been made at different shifted positions (l = 97; 99; 102; 105; 109; 112; 115; 118; 122; 125; 127 cm) and

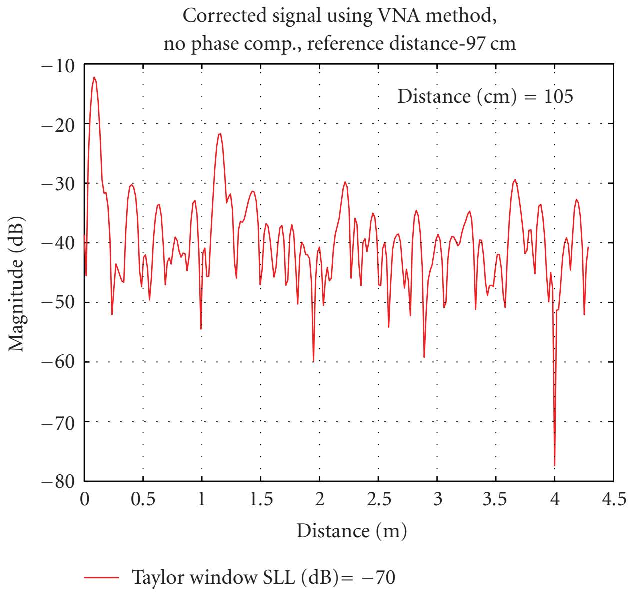

Figure 5: Calibrated *A*-scan using VNA method; reference distance-97 cm, separation 105 cm.

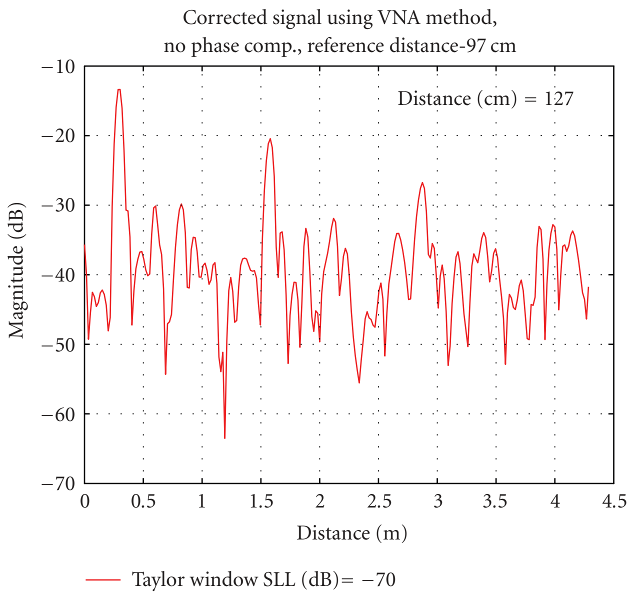

Figure 6: Calibrated *A*-scan using VNA method; reference distance-97 cm, separation 127 cm.

the unknown parameters are computed following a process of minimization of (10). The values obtained for the three unknowns are $u = 0.96888$; $v = 0.22 \times 10^{-10}$; and $w = 0$.

The results are presented in Figures 5 and 6. Comparing these figures with Figure 1, it can be seen that the time response decreases and the level of the signal just after the ground reflection is as low as −40 dB below the main peak. This outcome is quite important because the mines are supposed to be in this area.

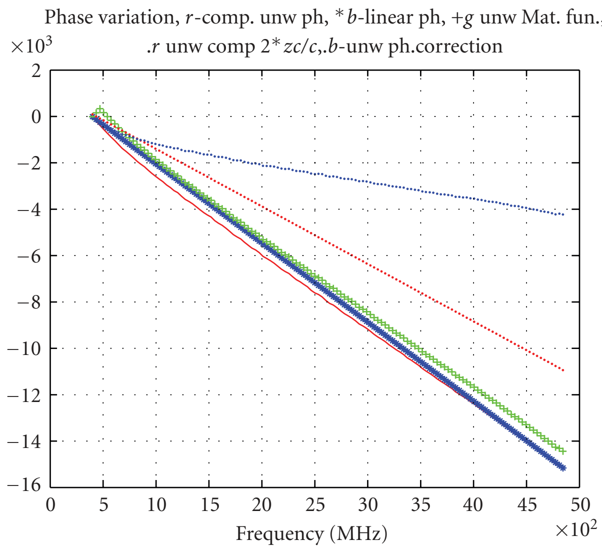

Figure 7: Unwrapped phase variation for 128 frequencies (light red: measured; dark blue: linearized; green: unwrapped with Matlab function; light red: due to propagation; light blue: phase error).

4. CALIBRATION PROCEDURE USING A METALLIC PLATE

The other procedure, which has been investigated, is the single reference procedure. It supposes to use a single reference, a metallic plate, located at a certain distance of the antenna system [5]. In this case, the transmitted signal is given by (1) and the received signal can be calculated using (2). As was mentioned before, the delays within the transmitting and the receiving antennas are frequency dependent. In fact, this effect can be seen in Figure 7 where the phase variation of the antenna is compared with a linear one. The upper line represents the phase distortion. As can be seen in Figures 1–3, there are multiple bounces so, in order to make a proper calibration, the first reflection should be isolated. Time domain gating can do this. In order to decrease the side lobes level, a Kaiser window, with $\beta = 3.15$, is applied.

The received signal after down conversion at the output of I and Q mixers will be

$$s(t_{in}) = \frac{1}{128}\sum_{n=1}^{128} r_n k_n A e^{-j2\pi f_n t_{in}}, \quad (11)$$

where k_n takes into accountthe variation of the gain along the processing chain for each frequency (channel). If the reference plate is located at a reference distance r_{ref} then the two-way propagation delay t_{ref} is given by

$$t_{\text{ref}} = \frac{2r_{\text{ref}}}{c}, \quad (12)$$

where c is the speed of light.

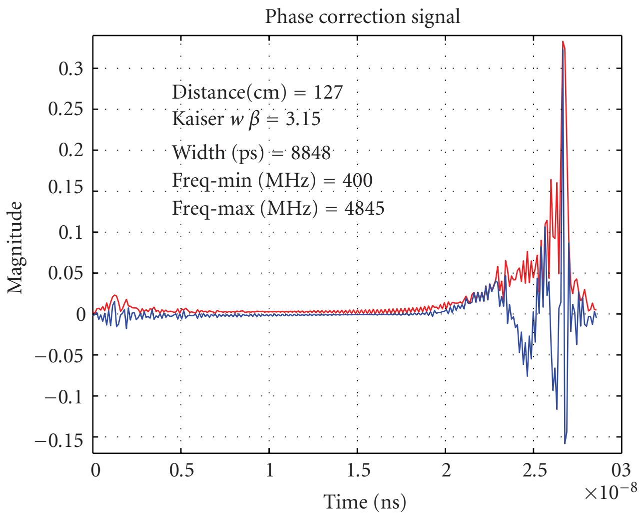

FIGURE 8: Phase correction signal in time domain (red line: absolute values, blue line: real values).

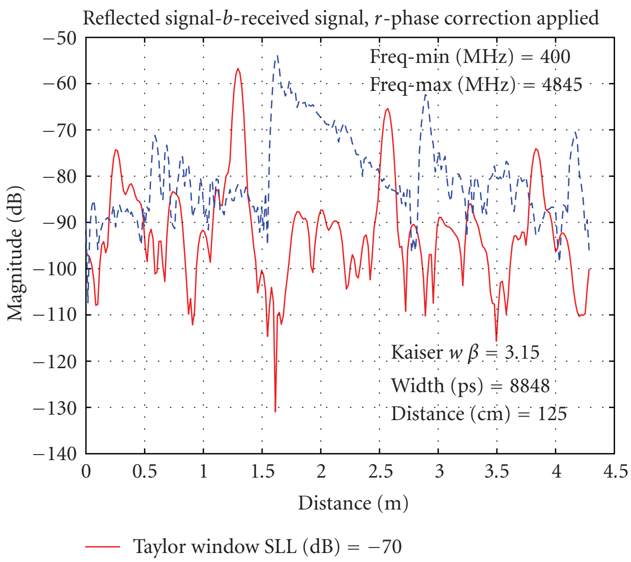

FIGURE 9: A range profile before calibration (blue line) and after calibration (red line) for a distance of 125 cm; data measured with VNA.

The correction signal that removes the phase dispersion within the antenna system will be

$$s_{cor}(t_{ref}, t_{in}) = \frac{1}{128}\sum_{n=1}^{128} e^{-j2\pi f_n (t_{ref}-t_{in})}. \quad (13)$$

This signal is displayed in Figure 8, in time domain, and it is the mirror image of the gated signal.

The calibrated signal is obtained by multiplying, for each frequency, the measured signal with the one given by (13). After an ifft is applied, a calibrated range profile as in Figures 9 and 10 is got. Matched filter calibration procedure has been employed for SFCW radar because the level of the side lobes in the vicinity of the ground reflection is lower than for VNA.

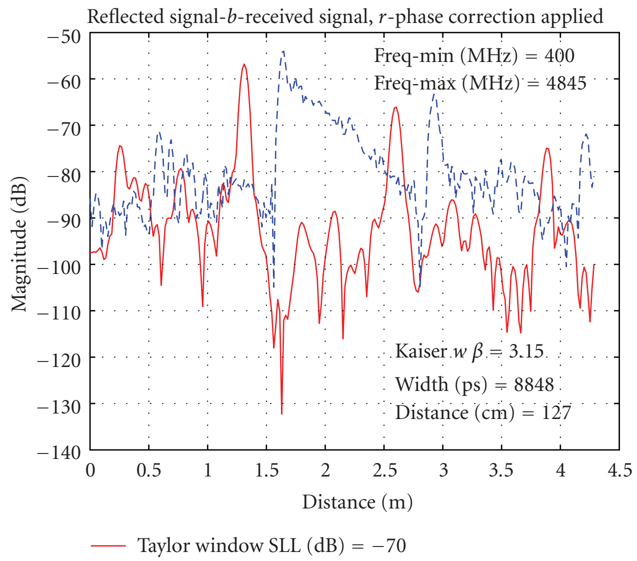

FIGURE 10: A range profile before calibration (blue line) and after calibration (red line) for a distance of 127 cm; data measured with VNA.

5. SYSTEM CALIBRATION

The SFCW radar works in frequency domain. After down conversion, at the output of the quadrature mixers, for each frequency, a complex signal is obtained. The phase and magnitude of these signals depend on the parameters of the processing chain and among these, the balance between I and Q channels plays a crucial role. The calibration of SFCW radar is made in two stages. In the first stage, the delays within the transmitter and the receiver are removed by making a direct connection, with a known length cable, between the two and dividing each A scan by this reference signal.

For one frequency, the output signal $s_1(f_k)$, after the first stage, is given by

$$s_1(f_k) = \frac{s_m(f_k) - s_{off}(f_k)}{s_{m\_ref}(f_k) - s_{off}(f_k)} e^{-j2\pi f_k (l_{ref}/v)}, \quad (14)$$

where $s_{off}(f_k)$ is the DC offset signal for the kth frequency, $s_{m\_ref}(f_k)$ is the measured signal with a direct connection between the transmitter and the receiver, $s_m(f_k)$ is the measured signal, l_{ref} is the length of the cable used for direct connection and v is the propagation velocity through the cable. The measured data, in time domain, after applying a Hamming window in order to decrease the side lobes level, are presented in Figure 11.

In the second stage, the single reference procedure is followed. To this end, a metallic plate is placed at 1.27 m separation of the antenna system. The performances that come out can be seen in Figures 12 and 13 where an uncalibrated and a calibrated A scans are showed. The first peak of the signal on Figure 13 is the coupling signal, the second is the reflection from the ground and the next are

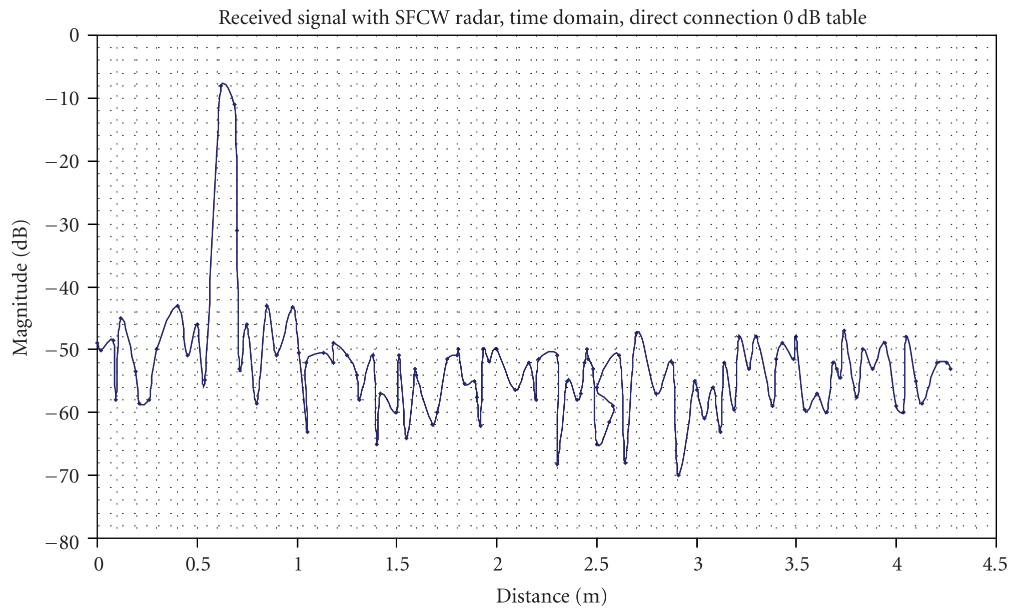

Figure 11: *A* scan (range profile) after removing the DC offset and the delays within the transmitter and the receiver.

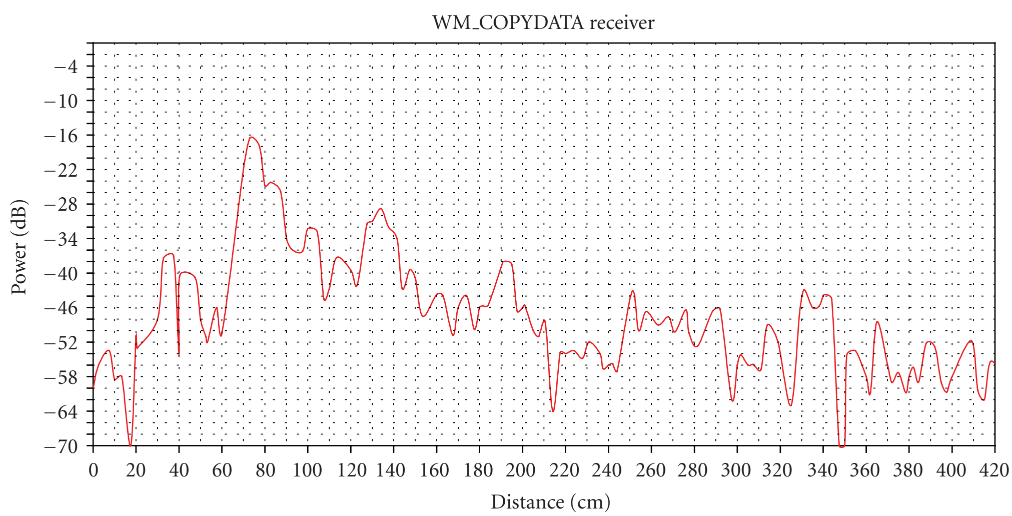

Figure 12: *A* scan measured with SFCW radar before calibration.

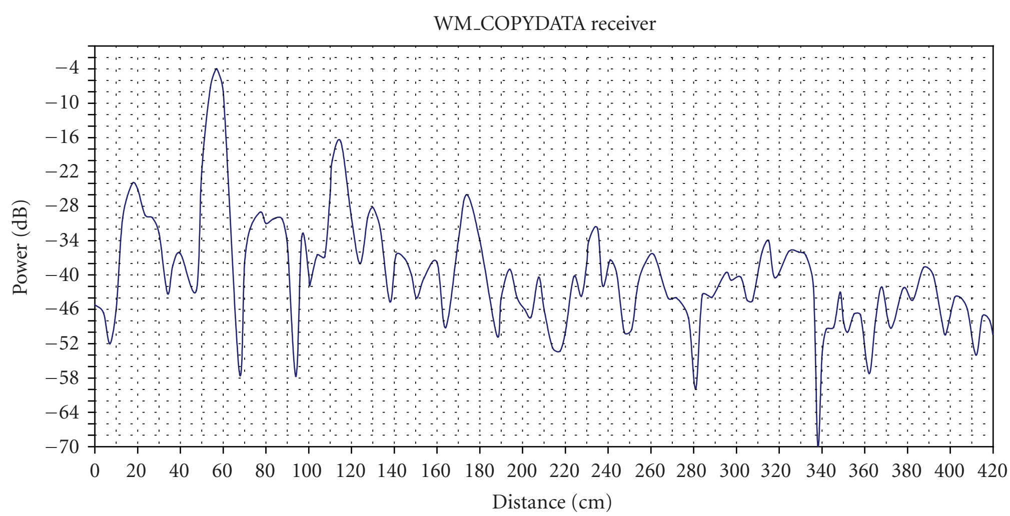

Figure 13: *A* scan measured with SFCW radar after matched filter calibration procedure is applied.

multiple bounces so, the third peak can be used as a measure of the RCS of the antenna system.

6. CONCLUSIONS

(1) The Archimedean spiral antenna is a very good candidate for UWB application but it has a major drawback because it is a dispersive system, which means that the delay within the antenna is frequency dependent. As a result, in any application where the shape of the pulse is important as, for instance in radar systems, a calibration procedure to remove the delays within the antenna system is needed.

(2) The SFCW radar works in frequency domain it means it has a synthesized time domain pulse that defines the downrange resolution of the system. The procedures described in the paper should be used to calibrate the system for the delays within the antenna system.

(3) For this application, because the landmines are supposed to be shallowly buried, the enlargement of the time domain response means that the reflection from the ground surface will cover the weaker signals, which may come from landmine. For the same reason, the level of the signal just after the first reflection from the ground has to be as low as possible.

(4) The three standards procedure that is used for the vector network analyzers calibration cannot be employed because of the difficulty to find a suitable standard besides the "empty room" and the metallic plate. Nonetheless, an alternative of this procedure, which supposes to replace the third standard with the same metallic plate but placed in a shifted position, has been analyzed. The side lobe level obtained with this procedure is just −40 dB below the main peak and is not enough for this application.

(5) The matched filter procedure needs a large separation between the antenna system and the reference plate in order to avoid the overlapping of the second reflection with the first one. Since the side lobes level near the ground reflection is decreased to around −50 dB (Figures 9 and 10), in comparison with VNA procedures that provides only −40 dB (Figures 5 and 6), this procedure is used for SFCW radar calibration.

(6) The Archimedean spirals work with circular polarization, which had been proven very useful for this application because it exhibits the shape of the detected object (the reflected signal embeds information about both dimensions of the object).

(7) The resolution of the SFCW radar is given by the time response of the system. As can be seen on Figures 12 and 13, it is improved from tens of cm to cm, which is in accordance with theoretical down range resolution given by the bandwidth of the radar.

REFERENCES

[1] D. J. Daniels, D. J. Gunton, and H. F. Scott, "Introduction to subsurface radar," *IEE Proceedings*, vol. 135, no. 4, part F, pp. 278–320, 1988.

[2] I. Nicolaescu, P. van Genderen, and J. Zijderveld, "Archimedean spiral antenna used for stepped frequency radar-footprint measurements," in *Proceedinngs of the Antenna Measurement Techniques Association (AMTA '02)*, pp. 555–560, Cleveland, Ohio, USA, November 2002.

[3] G. H. Bryant, *Principles of Microwave Measurements*, Peregrinus, London, UK, 1990.

[4] A. Al-Attar, J. Daniels, and H. F. Scott, "A novel method of suppressing clutter in very short range radar," in *Proceedings of the International Conference on Radar*, pp. 419–423, London, UK, October 1982.

[5] I. Nicolaescu, "Stepped frequency continuous wave radar used for landmines detection," Tech. Rep. IRCTR-S-004-03, Delft University of Technology, Delft, The Netherlands, 2003.


Journal of Engineering
The Scientific World Journal
International Journal of Rotating Machinery
Journal of Sensors
International Journal of Distributed Sensor Networks
Advances in Civil Engineering
Hindawi
Submit your manuscripts at
http://www.hindawi.com
Journal of Control Science and Engineering
Journal of Robotics
Journal of Electrical and Computer Engineering
Advances in OptoElectronics
VLSI Design
International Journal of Navigation and Observation
Modelling & Simulation in Engineering
International Journal of Aerospace Engineering
International Journal of Chemical Engineering
International Journal of Antennas and Propagation
Active and Passive Electronic Components
Shock and Vibration
Advances in Acoustics and Vibration